



Huang, Y., Mei, P., Lu, Y., Huang, R., Yu, X., Chen, Z. and Roskilly, A. P. (2019) A novel approach for Lithium-ion battery thermal management with streamline shape mini channel cooling plates. *Applied Thermal Engineering*, 157, p. 113623. (doi: [10.1016/j.applthermaleng.2019.04.033](https://doi.org/10.1016/j.applthermaleng.2019.04.033))

There may be differences between this version and the published version. You are advised to consult the publisher's version if you wish to cite from it.

<http://eprints.gla.ac.uk/257827/>

Deposited on 24 November 2021

Enlighten – Research publications by members of the University of Glasgow
<http://eprints.gla.ac.uk>

1 *A novel approach for Lithium-ion battery thermal*
2 *management with streamline shape mini channel cooling*
3 *plates*

4 Yuqi Huang ^a, Pan Mei ^a, Yiji Lu ^{a, b,*}, Rui Huang ^a, Xiaoli Yu ^{a, b},
5 Zhuolie Chen ^a, Anthony Paul Roskilly ^{a,b}

6 ^a *Department of Energy Engineering, Zhejiang University, Hangzhou, 310027, Zhejiang, China*

7 ^b *Sir Joseph Swan Centre for Energy Research, Newcastle University, Newcastle, NE1 7RU, UK*

8 **HIGHLIGHTS**

- 9 • Novel design method for the mini-channel cooling plate was proposed
- 10 • Distribution characteristics of typical and streamline shape channels were studied
- 11 • The efficiency of the mini-channel cooling plate could be significantly improved
- 12 • The flow resistance could be effectively reduced by the proposed solution

13 **Abstract**

14 The mini-channel cooling plate has been widely used in the Lithium-ion battery thermal
15 management for electric vehicles. The technology development of high efficiency and good
16 temperature uniformity cooling plate can promote the application of electric vehicles by
17 improving the lifespan of the battery. In this study, streamline concept, which is commonly
18 used for the external design of car, aerospace and submarine system to improve the system
19 performance, has been introduced to design and optimise the performance of inner mini
20 channel cooling plate. The flow resistance was proved to be minimised when the streamline

* Corresponding author.

E-mail address: luyiji0620@gmail.com (Y. Lu)

1 shape design was adopted. Moreover, the results have proven the novel designed mini
2 channel cooling plate can keep the heat exchange ability within the acceptable level. The
3 maximum improvement of the heat exchanger efficiency with streamline shape design could
4 be as high as 44.52 %. Results indicated the temperature uniformity could also be effectively
5 improved. The streamline shape mini channel cooling plate could be a promising solution for
6 Lithium-ion battery thermal management.

7 **Keywords:** Mini channel, Inner streamline shape, Battery thermal management, CFD
8 analysis, Electric vehicles

Nomenclature		P	static pressure (Pa)
A	surface area (m ²)	PCMs	phase change materials ()
C_{pw}	heat capacity of the liquid (J·kg ⁻¹ ·K ⁻¹)	PHEVs	Plug-in Hybrid Electric Vehicles ()
D_0	hydraulic diameter of the channel (m)	Pr	Prandtl Number ()
EVs	Electric Vehicles ()	q _a	heat flux (W·m ²)
f	non-dimensional surface friction factor ()	Re	Reynolds number ()
FCVs	Fuel Cell Vehicles ()	ΔT	temperature differences between the inlet and outlet (K)
G	mass flow rate (kg/s)	T	static temperature on the plate (K)
h	convective heat transfer coefficient (W·m ² ·K ⁻¹)	T _a	ambient temperature (K)
h_a	convective heat transfer coefficient of fluid (W·m ² ·K ⁻¹)	T_{avg}	averaged surface temperature via surface area (K)
HEVs	Hybrid Electric Vehicles ()	T _b	local temperature (K)
j	non-dimensional surface heat transfer ()	T_w	liquid temperature (K)
k	thermal conductivity of the fluid (W·m ⁻¹ ·K ⁻¹)	U_t	uniformity factor (K)
k_w	thermal conductivity of the liquid (W·m ⁻¹ ·K ⁻¹)	\vec{V}	velocity of the liquid (m/s)
L	characteristic dimension (m)	v _s	mean fluid velocity (m/s)
L_0	characteristic length (m)	Greek symbols	
L_1	entire flow distance (m)	μ	fluid viscosity (kg/m·s)
Nu	surface Nusselt number ()	ρ	fluid density (kg/m ³)
ΔP	pressure drop between the inlet and outlet (Pa)	ρ_w	density of the liquid (kg/m ³)

1 ***1. Introduction***

2 Increasing attention has been focusing on the environment problems and energy crisis, which
3 promote and lead the automotive industry to develop alternative technologies such as Electric
4 Vehicles (EVs) [1], Hybrid Electric Vehicles (HEVs), Plug-in Hybrid Electric Vehicles
5 (PHEVs) [2], and Fuel Cell Vehicles (FCVs) to potentially replace the existing Internal
6 Combustion Engine burning fossil fuels [3, 4].

7 The lithium-ion batteries are recognised as one of the best cell chemistries for EV, PHEV and
8 HEV [4, 5]. The advantages of lithium-ion batteries can be summarised as follows: 1) high
9 specific energy and power densities [3], 2) high nominal voltage and low self-discharge rate
10 [6], 3) long cycle-life and no memory effect [7]. However, in order to achieve enough
11 mileage equivalents to the conventional fossil-fuelled vehicle, EVs have to carry a large
12 number of battery cells. Therefore, it is critical and important to maintain lithium-ion
13 batteries operating under safety environmental conditions for EVs. During the discharging
14 process, Lithium-ion batteries generate a large amount of heat during the working process [8,
15 9], which may overheat the battery and induce some damages and accidents [10, 11]. In cold
16 weather, the battery performance also would be damaged when the circumstance temperature
17 is lower than at some particular level [12]. Thermal management systems are therefore
18 necessary and critical to control the battery temperature within an appropriate range, maintain
19 the temperature uniformity during the dynamical system operating [13-15].

20 Several thermal management systems were employed for battery packs, which also affect the
21 performance and cost of EVs [16]. There are many techniques have been widely applied and

1 discussed, such as forced convection with air [17-19] and liquids [18, 20, 21], phase change
2 material [22-24], heat pipes [25, 26], and the combinations by some of them [16]. The forced
3 convection air cooling technology suffers from the low thermal conductivity of the air [27],
4 which limits the cooling system performance. Moreover, the temperature difference between
5 the air inflow and outflow would induce the un-uniform in temperature distribution.
6 Compared with forced convection air cooling technology, the liquid system is more complex
7 but could offer higher ability by adopting a cold plate between the cells or submerging the
8 cell in a dielectric fluid [16]. Multi-mini-channel structures have been widely used in liquid
9 system working as heat sink or operating as cooling plates [28-30], which have been proved
10 as high efficient and compactable heat exchange structures. The commonly used heat transfer
11 mediums are mineral oil, water, refrigerants [31], dielectric fluid or ethylene glycol mixture.
12 The operating characteristics of the cold plate are mainly determined by the shape of the
13 channel, route, width and length [20, 21, 30]. Other technologies such as phase change
14 materials (PCMs) utilising the physical property of phase change to absorb and release heat
15 during a solid-liquid phase transition [32, 33] can also be used for electric vehicles thermal
16 management. When PCM such as the graphite matrix embedded paraffin wax is applied to
17 cooling the battery package, it also requires additional cooling system. Furthermore, it
18 enhances the additional weight and undesirable mass of the cooling system. Another
19 consequent of the large thermal mass and smaller heat transfer of the PCM technology leads
20 to low cooling rate [16]. The mechanism of the heat pipe is to transfer the heat through latent
21 heat of vaporization from the evaporator to the condenser, and the working medium can be
22 circularly motivated by capillary pressure developed within a porous wick lining [5]. Heat

1 pipes can cool or heat the battery efficiently, but they are similar to the passive strategy
2 offered by PCM. The combination of the heat pipe and air or liquid was proposed by Rao et
3 al.[14], but as a new and potential strategy applied to cool or heat battery pack, heat pipes
4 need to be further explored.

5 Many factors should be comprehensively considered in designing a liquid thermal
6 management system, such as space, weight, cost, potential leakage, efficiency, and the
7 thermal contact between the cold plate and cell [5, 25]. A cooling plate with excellent
8 performance is required to be in high efficiency, high uniformity, small size, low cost, and
9 lightweight. Computational fluid dynamics (CFD) is commonly used and recommended for
10 design and optimisation because of the advantages such as low cost and flexibility [5]. Zhao
11 et al. designed a cooling strategy for cylindrical batteries based on a mini-channel liquid and
12 applied the numerical model to investigate the variation of the channel quantity, mass flow
13 rate, flow direction and entrance size [34]. Huo et al. developed a 3D thermal model of the
14 cooling system and studied the effects of flow direction, inlet mass flow rate, number of
15 channels and ambient temperature on temperature increase and distribution of the battery
16 during the discharge [35]. The study reported by Huo et al. [35] investigated the influence of
17 channel numbers on the cooling plate. The results pointed out when water was directed flow
18 into the channels on the side of the electrodes, the best cooling performance could be
19 achieved. However, the cooling plate from previously reported work only considered straight
20 and parallel channels. The methods of flow separation from the main supplied channel and
21 the pressure drop between the inlet and outlet of the cooling plate require further

1 investigations and research efforts. In summary, the detailed structure of the channel was
2 found to be a key factor which directly affected the heat exchange efficiency. Since the area,
3 thickness, inlet and outlet position of cooling-plate were restricted by the whole package
4 design in most conditions, the optimizing direction would be focused on improving the
5 structure of channels. Therefore, the research goal of this study is to achieve high efficiency
6 and temperature uniformity by optimising the design of the channel structure.

7 In this work, streamline concept, which is commonly used for the external design of car,
8 aerospace and submarine system to improve the system performance was introduced into
9 mini channel cooling plate to optimise the heat exchanger performance in the inner flow field.
10 The design methods of the streamline shape mini channel have been first introduced and
11 described. The proposed methods can be applied for different cooling plates with the
12 potential to reduce the inner flow resistance of heat exchanger, maintain the heat dissipation
13 ability of the mini-channel heat exchanger for the application of electric vehicle battery
14 thermal management.

15 ***2. Methodologies***

16 ***2.1 Description of the mini-channel plate model***

17 The battery package used in the electric vehicle usually composes of thousands of battery
18 cells in order to meet the power demand. The battery cells are assembled into several battery
19 modules. Each battery module is attached with several cooling plates to control the thermal
20 conditions. When the shape of the battery is rectangular, the cooling plates can be inserted

1 into the gap of adjacent batteries. The inner temperature of the module is monitored and
2 adjusted by controlling the liquid temperature and mass flow rate.

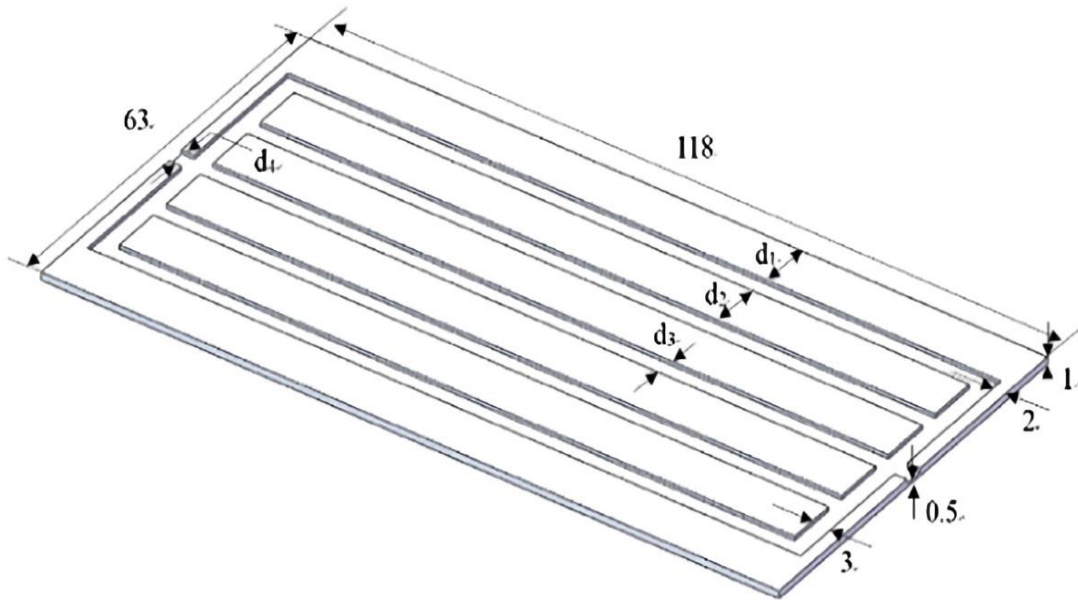


Fig.1. Schematic structure of the cooling plate [36]

3 A multi-channel plate with a typical structure as reported by Qian Z et al.[36] has been
4 selected as the research object in this study. The width of all the gaps d1, d2, d3 and d4 of the
5 plate are 3 mm as shown in Fig 1. And the height of the channel is 1mm. Some other plates
6 which have the same outside size with a different number of channels (from 3-7) and the
7 optimisation methods through the novel design method are also discussed in this paper.

8 **2.2 Control equations**

9 According to the theory of heat transfer, a convective boundary condition exists at each of the
10 battery's outer walls. Newton's Law of Cooling suggests that the amount of heat dissipated
11 due to the movement of a fluid can be found using Eq. (1), where T_a (K) is the ambient
12 temperature. h_a ($W \cdot m^{-2} \cdot K^{-1}$) is the convective heat transfer coefficient of fluid.

$$q_a = h_a(T_b - T_a) \quad (1)$$

1 The heat transfer fluid (water-ethylene glycol mix) was employed as the cooling medium.
 2 The energy conservation equations for the liquid within the cold plate channels are calculated
 3 by Eq. (2), where ρ_w (kg/m³), c_{pw} (J·kg⁻¹·K⁻¹) and k_w (W·m⁻¹·K⁻¹) are the density, heat
 4 capacity and thermal conductivity of the liquid, respectively. T_w (K) is the liquid temperature
 5 and \vec{v} (m/s) is the velocity of the liquid.

$$\frac{\partial}{\partial t}(\rho_w c_{pw} T_w) + \nabla \cdot (\rho_w c_{pw} \vec{v} T_w) = \nabla \cdot (k_w \nabla T_w) \quad (2)$$

6 The mass and momentum conservation equations can be written as the following two
 7 equations, where P (Pa) is the static pressure.

$$\frac{\partial \rho_w}{\partial t} + \nabla \cdot (\rho_w \vec{v}) = 0 \quad (3)$$

$$\frac{\partial}{\partial t}(\rho_w \vec{v}) + \nabla \cdot (\rho_w \vec{v} \vec{v}) = -\nabla P \quad (4)$$

8 **2.3 Parameters**

9 j/f is a non-dimensional factor [37, 38], which has been widely used in the heat exchanger
 10 to evaluate the comprehensive performance of the plate. The factor j represents the
 11 non-dimensional surface heat transfer, which can be calculated by Eq. (5). Nu is the
 12 surface Nusselt number, equals to hL_0/k , where h (W·m²·K⁻¹) is the convective heat transfer
 13 coefficient, L_0 (m) is the characteristic length and k (W·m⁻¹·K⁻¹) is the thermal conductivity
 14 of the fluid. Re is the Reynolds number in the channel. Pr is the Prandtl Number, which
 15 is a taken as constant number (6.22, the Prandtl number when the water at 298K).

$$j = \frac{N_u}{R_e \cdot P_r^{1/3}} \quad (5)$$

1 f is the non-dimensional surface friction factor, reflects the flow resistance internal of the
 2 channels. Which could be calculated by Eq. (6) where D_0 (m) is hydraulic diameter of the
 3 channel, ΔP (Pa) is the pressure drop between the inlet and outlet, L_1 (m) is the entire flow
 4 distance, G (kg/s) is the mass flow rate, and ρ (kg/m³) is the fluid density.

$$f = \frac{D_0 \Delta P}{4L_1 G^2 / 2\rho} \quad (6)$$

5 U_t is the uniformity factor, which is used to evaluate the uniformity of temperature
 6 distribution, which could be calculated by Eq. (7) [39, 40].

$$U_t = \frac{\int_A |T - T_{avg}| d_A}{\int_A d_A} \quad (7)$$

7 T_{avg} (K) means the averaged surface temperature via surface area, could be written as Eq. (8),
 8 where A (m²) is the surface area and T (K) is the static temperature on the plate.

$$T_{avg} = \frac{\int_A T d_A}{\int_A d_A} \quad (8)$$

9 **2.4 Numerical analysis**

10 The three-dimensional cooling plate model has been numerical analysed in ANSYS FLUENT
 11 17.0. Before the numerical simulation, the model was discretized by HYPERMESH 14.0.

1 The local hexahedral mesh was generated in a boundary layer, seven type of hybrid grids
 2 with the cell number from about 38 thousand to 2.92 million were developed as listed in
 3 Table 1. In the simulations, water-ethylene glycol has been used as the cooling medium
 4 through the channels. The mass flow rate was set as constant at $1 \times 10^{-3} \text{ kg} \cdot \text{s}^{-1}$, the uniform inlet
 5 temperature was set at 298K. The material of the solid plate is Aluminium, and the constant
 6 heat flux condition was applied in the large top and bottom faces of the cooling plate.
 7 Reynolds number could be calculated by the mass flow rate define at the cooling channel
 8 inlet to confirm the use of a viscous model, which is defined as shown in Eq. (9), where v_s
 9 (m/s) is the mean fluid velocity, L (m) is the characteristic dimension, μ (kg/m-s) is the
 10 viscosity, ρ (kg/m^3) is the fluid density.

$$R_e = \frac{\rho v_s L}{\mu} \quad (9)$$

11 The maximum mass flow rate was set at $5 \times 10^{-3} \text{ kg} \cdot \text{s}^{-1}$, which corresponds to a Reynolds
 12 number less than 2300. Since the flow was laminar, the laminar model and SIMPLEC
 13 algorithm were used with second and third order equations.

14 **Table 1**

15 Grid type and corresponding cell number

Type	Grid 1	Grid 2	Grid 3	Grid 4	Grid 5	Grid 6	Grid 7
Cell Number	38809	90658	192067	470325	882117	1355279	2921580

16 In order to identify proper grid number, the independent study of grid number through the
 17 comparison of pressure drops and temperature differences has first been conducted. Fig.2
 18 displays the results under different grid number. The grid type and corresponding cell number

1 are listed in Table 1. The results indicated when the grid numbers reach to about 0.88 million,
 2 the fluctuations of both ΔP and ΔT induced by the difference of grids number were less than 3%
 3 (actually is only around 2%) even the grid number was further increased. Therefore the Grid
 4 5 and corresponding mesh generating rules were selected as the final scheme in this study.
 5 The local display of the grids is shown in Fig.3.

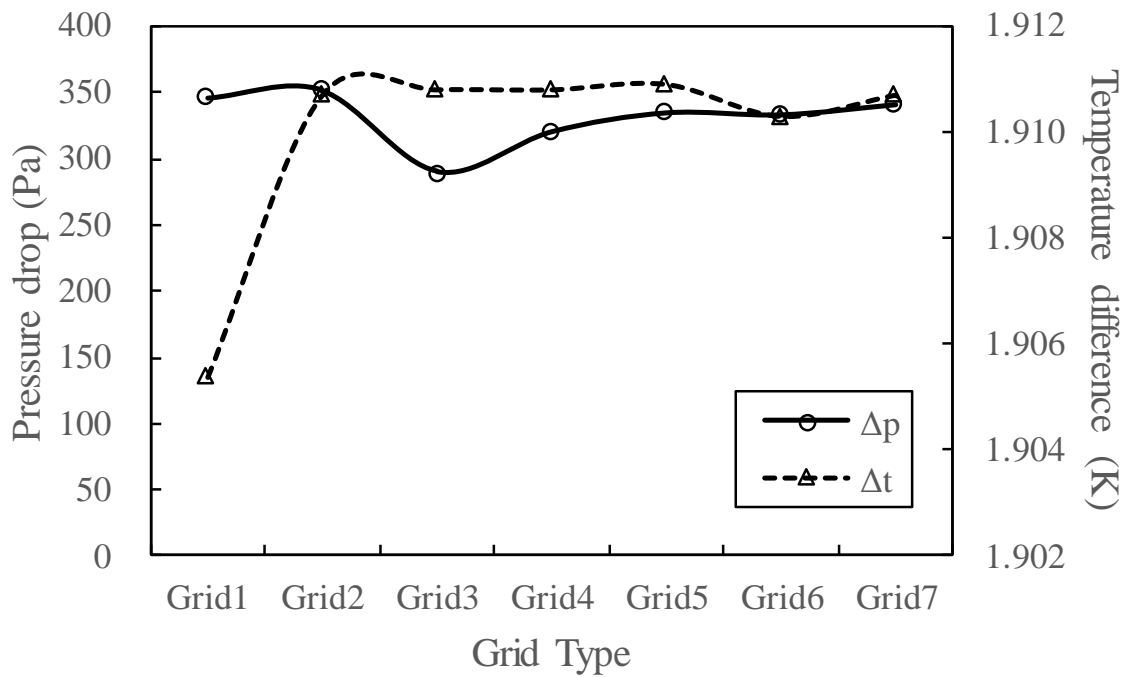


Fig.2. Effects of grid number on the pressure drops and temperature differences

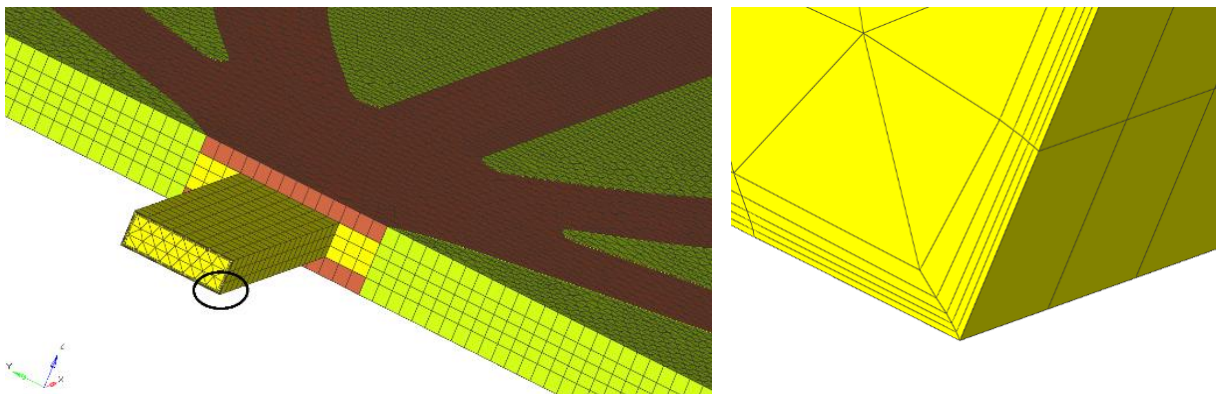


Fig.3. Local display of the grids

6 **2.5 Validation**

1 To validate the simulation results, six three-dimensional simulation models are established
2 and discretized by the rules discussed previously. The results are compared with the reported
3 data from the literature as illustrated in Fig. 4.

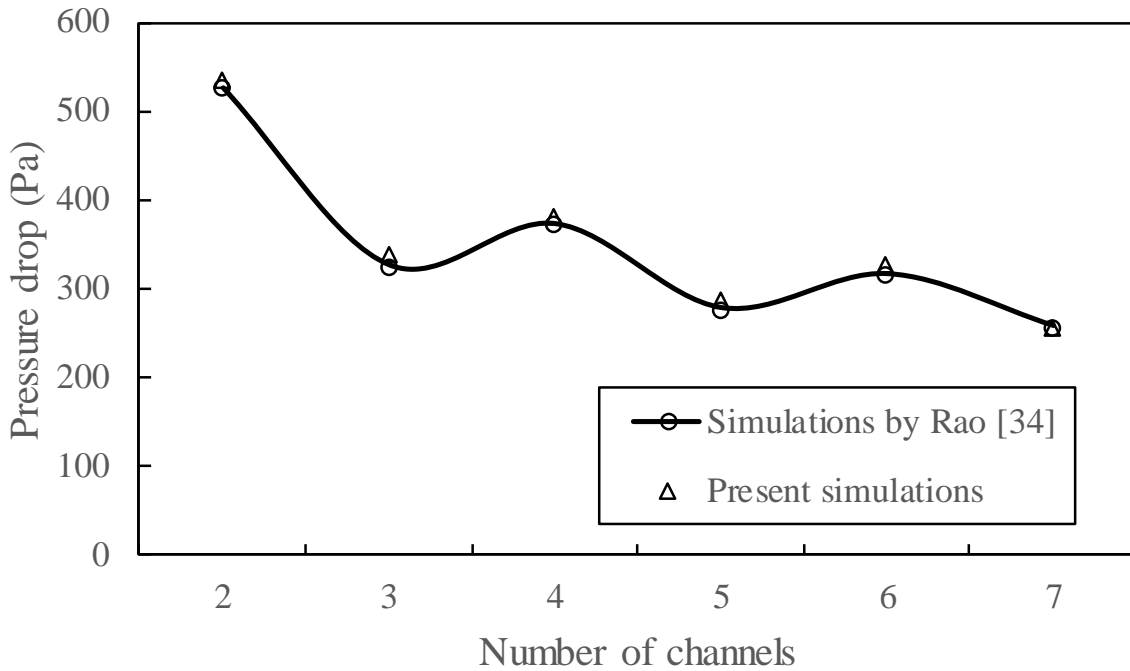


Fig.4. Comparison of the numerical simulation results with literature

(mass flow rate = 0.001kg/s)

4 The calculated pressure drop can be well fit with results reported by Rao [34]. The maximum
5 error is less than 4.5%, which proves the numerical simulation methods applied in this paper
6 are acceptable and reliable. The results indicated that the pressure drops in plates with even
7 number channels are much higher than the one in odd number channels plate.

8 ***3. Design methods***

9 Multi-channels structure has been widely used in cooling-plate, the effects induced by some
10 parameters such as the number of channels, mass flow rate and flow direction have been
11 previously discussed [25]. However, the study of channel shape and corresponding influence

1 on the mini-channel plate have not been noticed and reported. With the development of
2 technology, the design and manufacture of the non-straight channel can be achievable. The
3 design procedure of internal streamline concept for multi mini channel plates can be
4 described as follows,

- 5 1. Determine the outside structure of the plate by objective conditions. The length,
6 width, thickness, the location of the inlet and outlet are usually restricted by the
7 spatial structure of the battery module. The plate shown in Fig.5 (a) is taken for
8 example. Presuming the whole plate is an empty flow field, only the inlet, outlet, and
9 the plate are modelled.
- 10 2. Decide the boundary conditions through the estimation of working conditions,
11 simulating the flow status of this plate. For example, the mass flow rate could be
12 calculated through the pump lift and the number of cooling plates or through the
13 cooling capacity required of the batteries under the maximum heat release.
- 14 3. Extract the streamlines in the flow field of the plates by post-processing tools.
15 According to the targeted channel number, extract the streamlines. The extract rule
16 could be equidistant or adjust the spacing of streamlines according to the local flow
17 rate. In Fig.5 (b), the streamlines are extracted equidistant.
- 18 4. Expand the shape of streamlines to and the streamline-shape channels can be formed
19 as illustrated in Fig.5 (c).

- 1 5. Develop a three-dimensional model with the streamline-shape channel, as shown in
- 2 Fig.5 (d). Both step 4 and step 5 could be carried in CAD software, CATIA or
- 3 SOLIDWORKS.

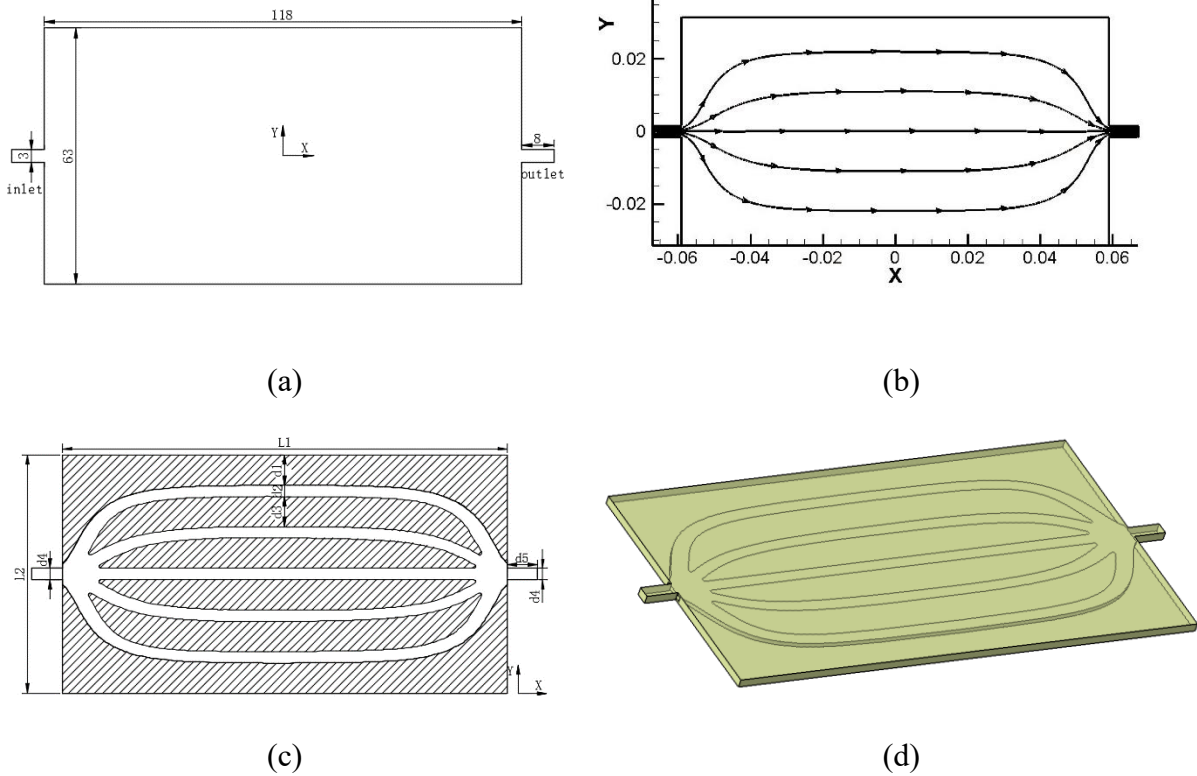


Fig.5. The schematic of the novel channels design procedure (a) the empty plate (b) extracted streamline (c) build the channels in 2D (d) 3-Dimensional channels

4. Results and discussion

4.1 Distribution characteristics of the typical straight and streamline shape channel plate

Five different plates with 3, 4, 5, 6, 7 channels were developed to investigate and compare the performance of the cooling plate with conventional shape channel and streamline shape

1 channel. All the plates were numerically studied, and the results were compared with the
 2 simulating results under the same boundary conditions. The cooling plates with streamline
 3 shape channel were named as S3, S4, S5, S6 and S7. The plates with typical rectangular
 4 shape are named O3, O4, O5, O6 and O7. The mass flow rates of 0.001kg/s, 0.002kg/s,
 5 0.003kg/s, 0.004kg/s, and 0.005kg/s were analysed.

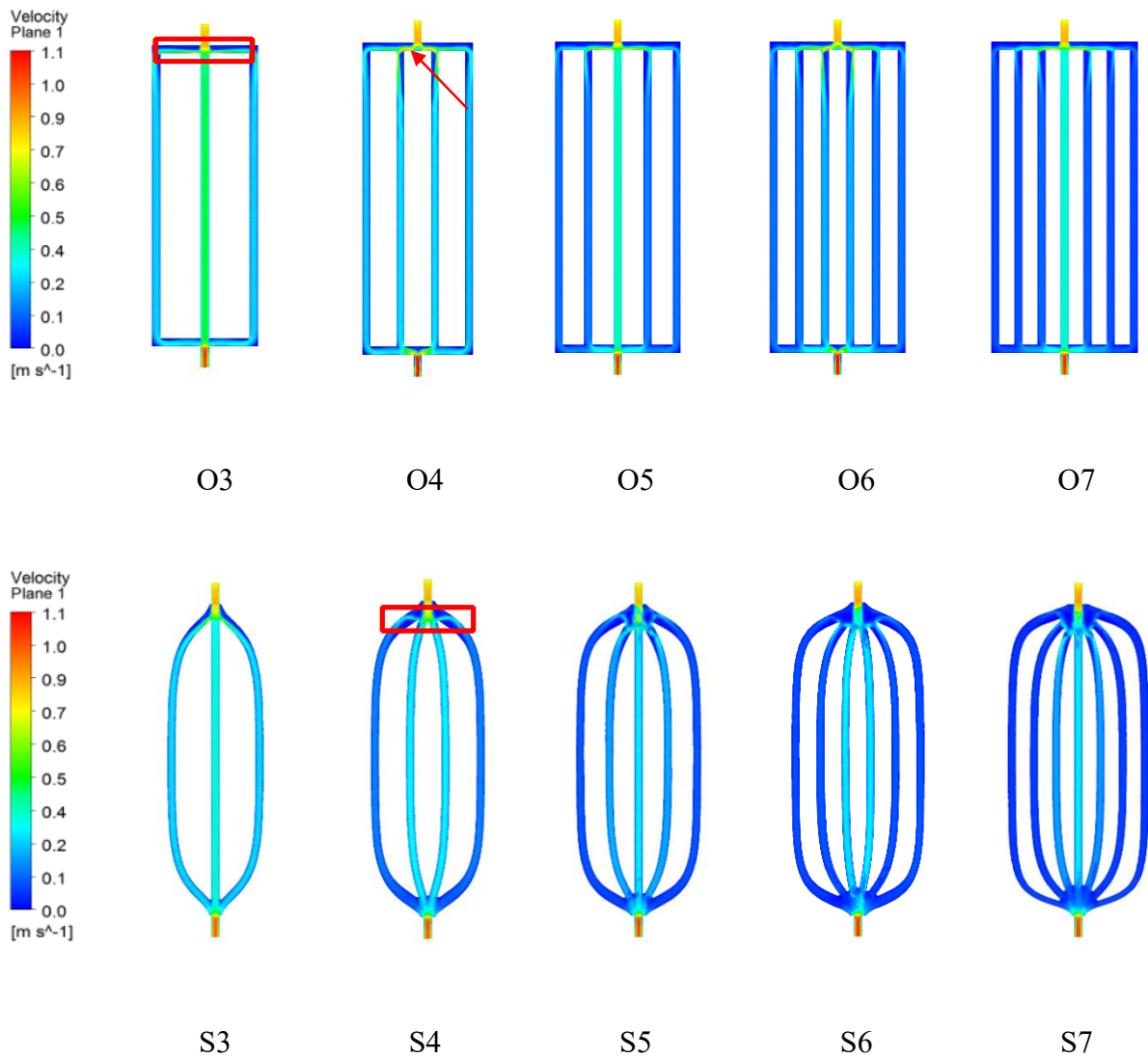
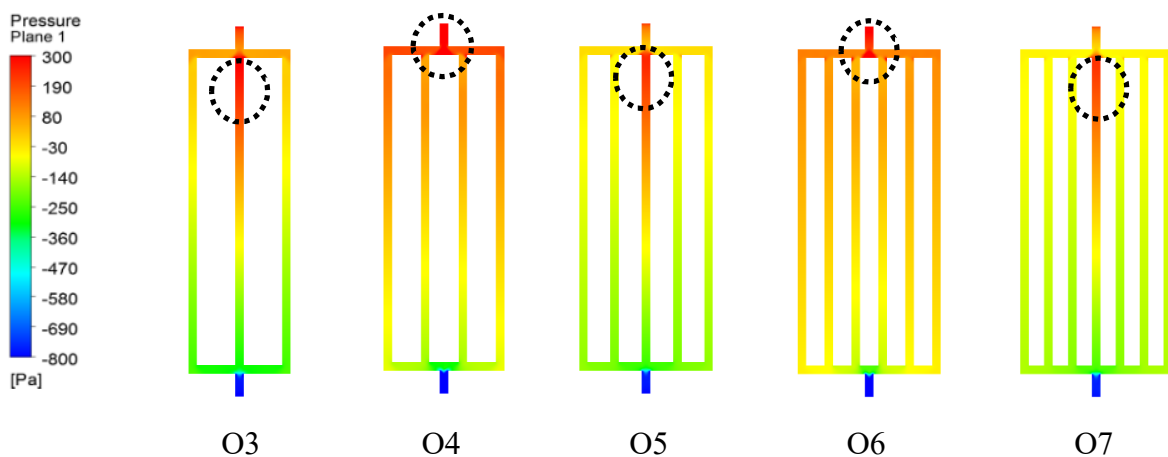


Fig. 6. The comparison of flow velocity distribution in channels

(mass flow rate = 0.002kg/s)

1 Fig.6 compares the velocity contours in channels of different plates. In all the straight
2 channel models, the water flow impacts to the lower wall of the upper horizontal channel
3 accelerate the flow along to the lower wall. The layered velocity could be observed in all
4 straight channel models. For even number channel models, very high velocity in the local
5 of horizontal channel close to the inlet of two middle channels can be observed, as
6 marked by the red arrow O4 shown in Fig. 6. Some vortex and turbulence flow might be
7 generated in this area, which would increase the flow resistance and has a bad effect on
8 the performance of the cooling plate. By adopting the streamline shape channel, the flow
9 velocity can be effectively reduced in the same area, which means the vortex and
10 turbulence flow can be avoided to improve the cooling plate performance. For odd
11 number channel models, the difference of velocities between the middle channel and
12 other channels is quite high in straight channel models. The velocities of streamline
13 channel models with odd number channels are lower than that of straight channel models,
14 which are desirable for the cooling plate.



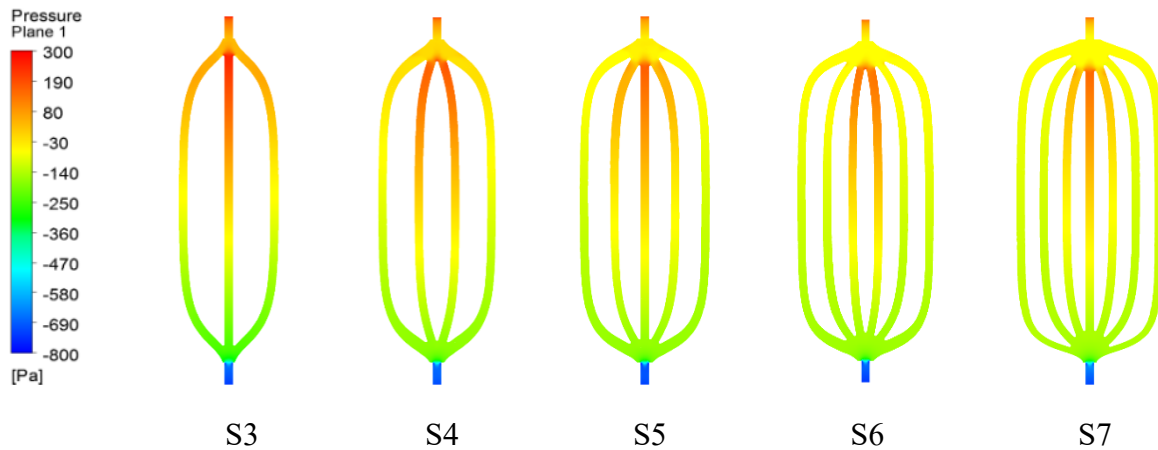


Fig. 7. The comparison of pressure distribution at the mid- profile of channels
(mass flow rate=0.002kg/s)

1 Fig. 7 shows the pressure contours in all the models. In straight channel plates, the high
 2 pressure appears at the middle channel (odd channels plate) or the inlet tunnel (even
 3 channels plate) as circled by dashed lines. By comparing the colour distribution, the
 4 pressure could be effectively reduced by adopting the streamline design of channel shape,
 5 which means the entire flow resistance would be minimised. As illustrated in Fig. 7 in
 6 the models with even channels (4 channels and 6 channels), the high-pressure regions are
 7 observed in the top horizontal channels for straight channel models and when the
 8 streamline channel models are used, the pressure values can be effectively decreased
 9 since the colour changes from red to orange under the same pressure regions of straight
 10 channel models. As illustrated in Fig. 6 and Fig. 7, it could be noticed that there are two
 11 main factors which induce flow resistance in even channels. First, the flows turn around
 12 sharp corner. Second, the flows need to be separated from inlets. The first factor could be
 13 effectively avoided by using the streamline channels. The second factor requires
 14 optimisations on the separating zone.

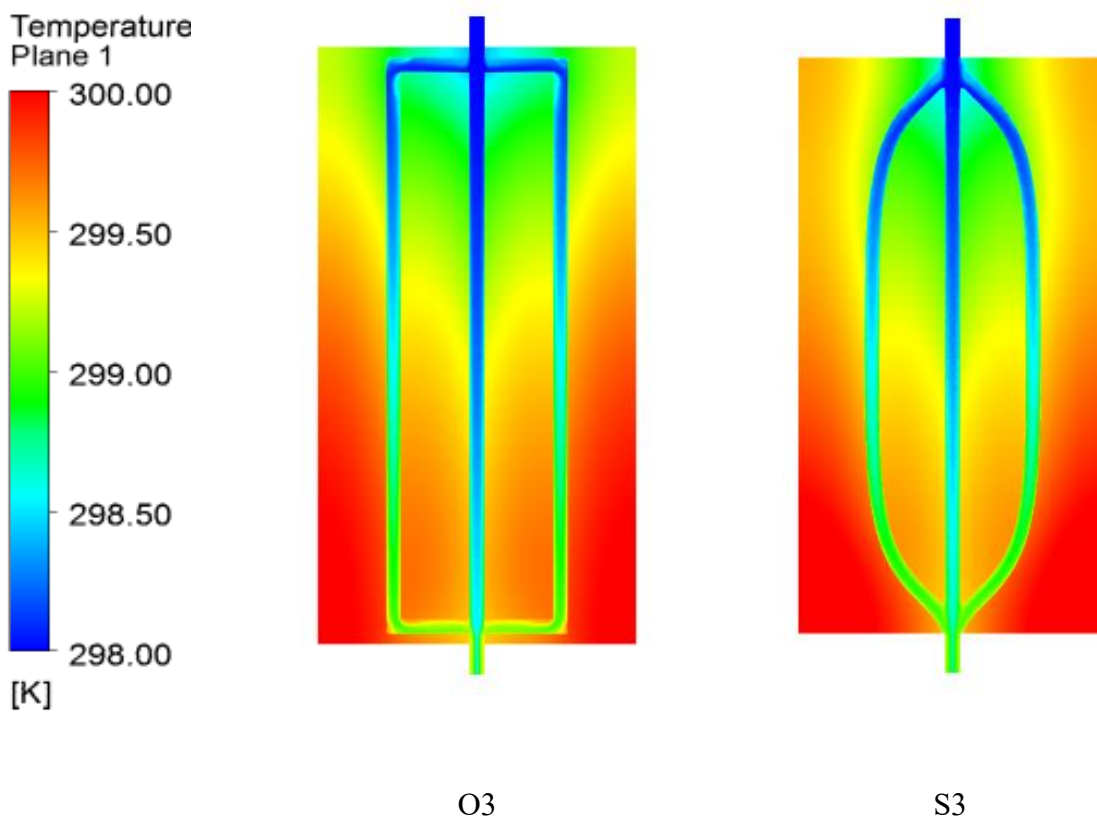


Fig.8 The comparison of temperature distribution at the mid- profile of plates

(mass flow rate=0.002kg/s, three channel)

1 Fig.8 compares the temperature distribution at the mid-profile of plates when the mass flow
 2 rate is 0.002kg/s to study the cooling ability of these plates. The cooling performance of three
 3 channel shapes could be identified through the colour since all legends are same. The
 4 temperature in the up corner of plates with straight channels is slightly lower than the one in
 5 the plates with streamline shape channels as illustrated in Fig. 8. The temperature of the
 6 cooling medium in the outlet are quite similar in both models. The difference in velocity,
 7 pressure and temperature conditions using the typical straight channels and streamline shape
 8 channels can be observed in Fig. 6, 7 and 8, which can help to study the inner flow and
 9 thermal status. The study of distribution characteristics not only can be used as the assistant

1 reference for validation of the numerical simulation results but also be helpful to summarise
 2 the optimal strategies.

3 **4.2 Effects of channel structures on the cooling plate performance**

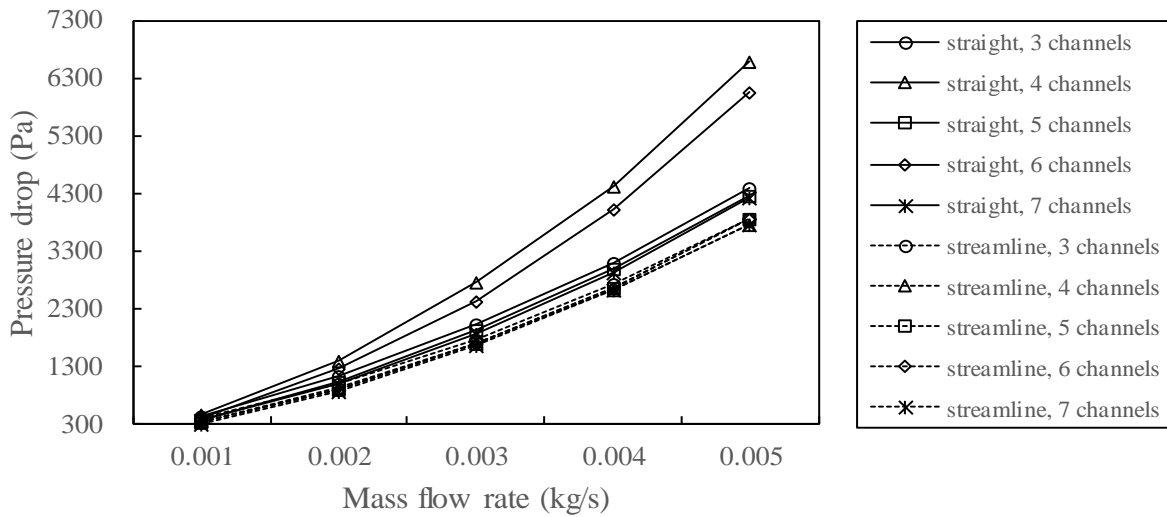


Fig.9. Effects of mass flow rate on the pressure drop of different plate models

4 The pressure drop of different plates is plotted in Fig.9. Under the same mass flow rate, the
 5 pressure drop in streamline models is significantly less than the pressure drop in the typical
 6 straight channels. For the typical straight channel models, the flow resistance in the plates of
 7 even number channels is always higher than that of plates with an odd number of channels.
 8 However, when the streamline shape channels are used, the maximum pressure drop as
 9 indicated in Fig 9 is only 3877 Pa under mass flow rate at 0.005 kg/s, which is much lower
 10 than that of typical straight plate models. The results also indicate the effects of channel
 11 numbers on the pressure drop for streamline shape channel models is quite limited and the
 12 pressure difference with different channel numbers is lower than 100 Pa. This phenomenon

1 can also be observed with the assistant of a distribution diagram in Fig. 7, which shows flow
 2 impaction to the tunnel wall when the even number channels are used. When the mass flow
 3 rate is 0.005 kg/s, the pressure drop can be as high as 6581 Pa and 6043 Pa with four and six
 4 typical straight channel number, respectively. The difference between the pressure drops of
 5 typical straight channel models with three and seven channels is as high as 2350 Pa under the
 6 mass flow rate at 0.005 kg/s. The results in Fig. 7 and Fig. 9 have proven the streamline shape
 7 channels can effectively reduce the pressure drop and avoid the direct flow impaction.

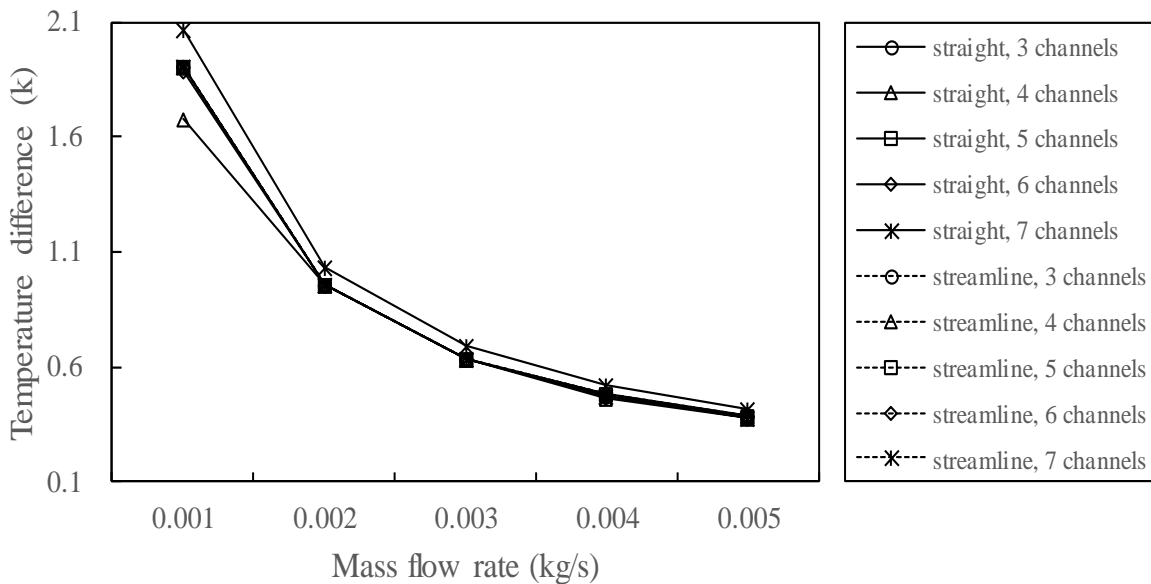


Fig.10. Effects of mass flow rate on temperature difference (cooling ability) of different plate models

8 The temperature difference using different models have also been investigated under different
 9 mass flow rate and the results are plotted in Fig. 10. The investigation of temperature
 10 difference can be used to evaluate the cooling ability of the mini-channel cooling models.
 11 Results indicate the straight 7 channels model has the best cooling ability, which is coincident

1 with the results calculated by Rao [33]. Results indicate the maximum temperature difference
 2 is 2.07 K achieved by straight 7 channel model when the mass flow rate of the fluid is at
 3 0.001 kg/s and under the same conditions, the worst cooling ability is observed by straight 4
 4 channel model who can only achieve 1.68 K temperature difference. When the streamline
 5 shape channels are used, the temperature difference of the models with different numbers of
 6 the channel is quite similar to that of typical straight 5 channel model, which means the
 7 streamline channel models can keep the cooling ability in the same standard as the typical
 8 straight channel model. In summary, by introducing the concept of streamline into mini
 9 channel cooling plate, not only the pressure difference can be effectively reduced, but also the
 10 effects of different numbers on the cooling ability can be controlled.

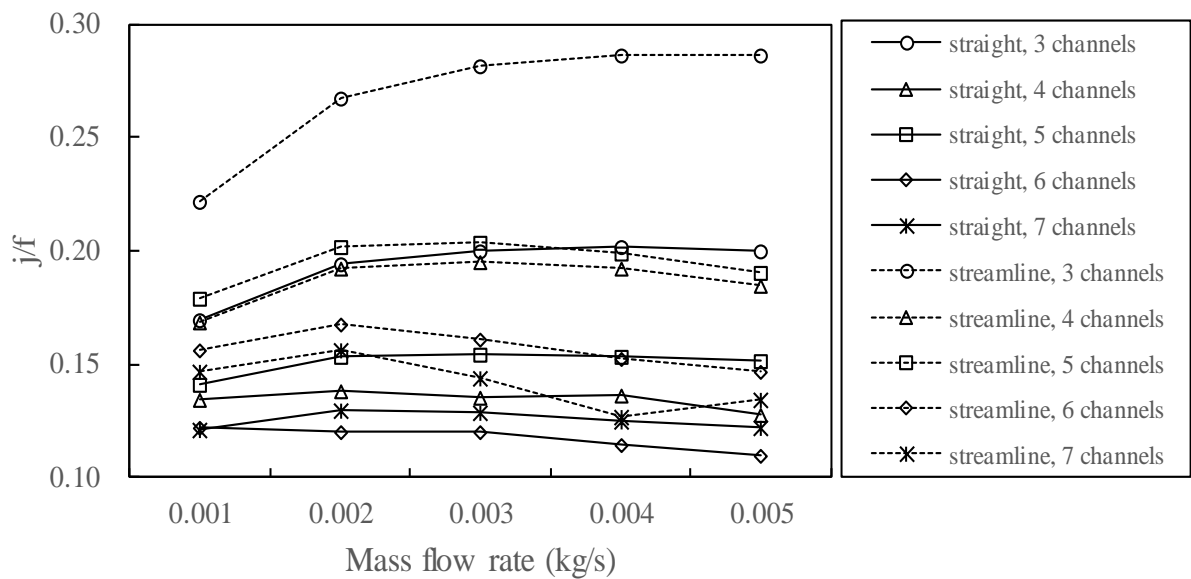


Fig. 11. Effects of mass flow rate on the j/f factor of different plate models

11 Fig.11 displays the j/f factor of different plates at various mass flow rates. j/f factor
 12 has been adopted to evaluate the efficiency of the heat exchanger. Both the heat exchange

1 capacity and the flow resistance are taken into consideration in this factor. j/f factor in
 2 plates with streamline shape channels are significantly higher than that of typical straight
 3 channel models. With the increase of channel number, the difference between j/f factor is
 4 reduced, which means under high channel numbers the improvement of heat exchanger
 5 efficiency is limited by introducing the concept of streamline shape model into cooling plate
 6 technology. The streamline 3 channel model has the highest. For straight models, 6 channel
 7 model has the lowest j/f factor, which means the efficiency of it is the worst. However,
 8 for streamline models, 6 channel model is better than the 7 channel model, which prove the
 9 streamline design could restrain the flow resistance effectively as previously discussed.

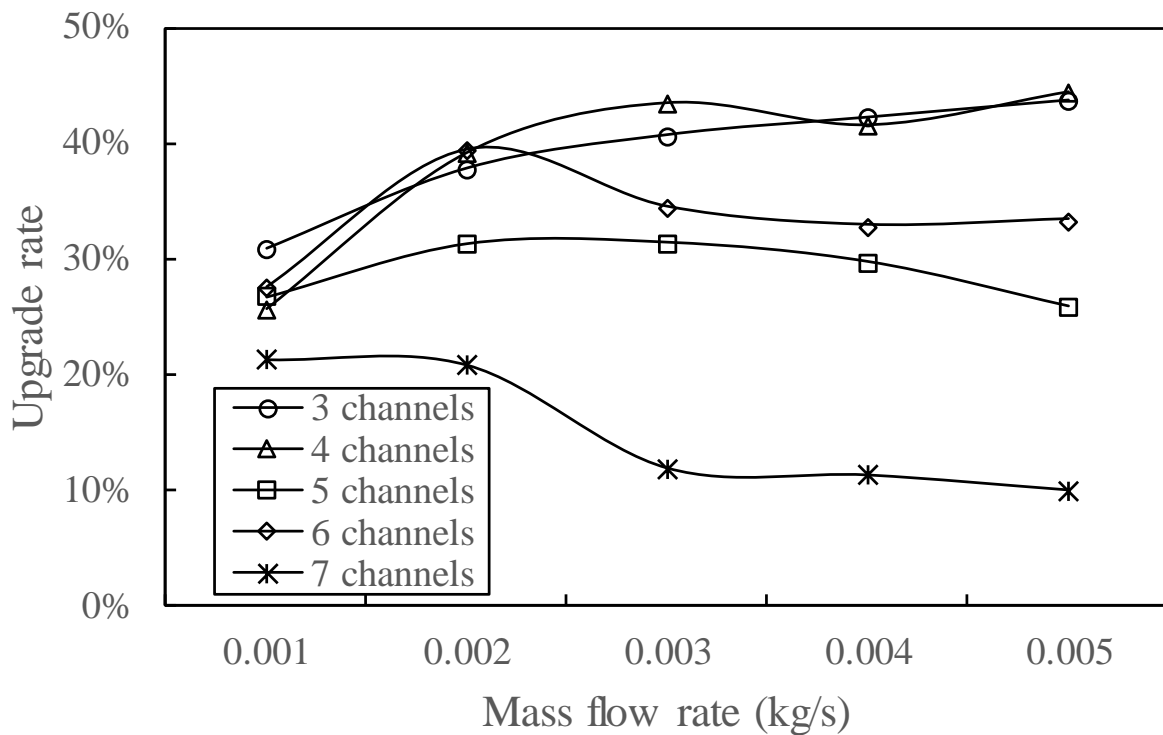


Fig. 12. The upgrade rate of j/f factor under different mass flow rates

1 Compare the j/f factor of streamline models and straight models, the upgrade rate could
 2 be calculated as shown in Fig. 12. When the number of channels is 3, the streamline shape
 3 model can improve the j/f factor by 44.52% as shown in Fig 11. When the channel
 4 number is seven, the streamline shape model can improve the j/f factor by 10.08 %.
 5 When the mass flow rate is around 0.002kg/s, the improvements in 4 & 6 channel model are
 6 notably high. It might because the streamline shape is extracted from the flow field, which
 7 would be affected by flow velocity. If the current flow characteristics matching the channel
 8 shape coincidentally, the efficiency could be further increased.

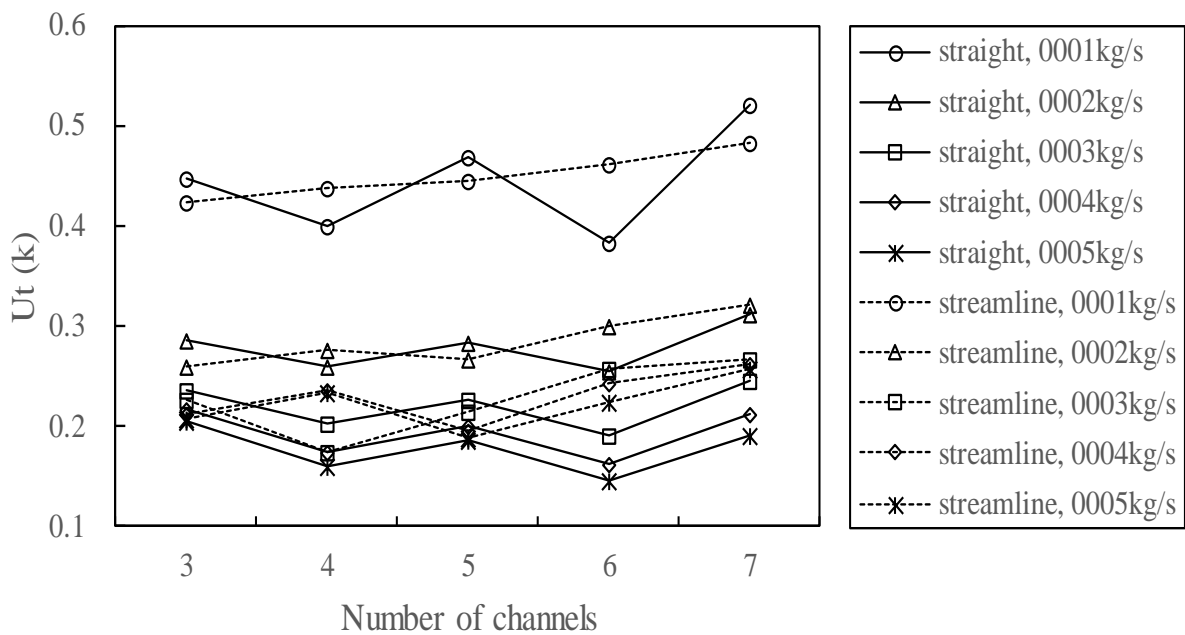


Fig.13. The uniformity factor under different mass flow rates

9 The temperature uniformity is also a very important factor for battery thermal management.
 10 The uniformity factor U_t is adopted to study the temperature uniformity in the middle
 11 profile of plates. Fig.13 compares the uniformity factor of models at different mass flow rates.
 12 When the mass flow rate increased, the uniformity decreased accordingly. When the mass

1 flow rate is operating at low range such as 0.001 and 0.002 kg/s, the temperature uniformities
2 in straight channel models with odd numbers have better performance than that of streamline
3 channel models. However, when the channel numbers are even, the temperature uniformities
4 in streamline models are significantly improved than that of straight channel models under
5 the same mass flow rates. With the increase of channel numbers, the streamline models
6 exhibit good uniformity. With further optimisation of the design of streamline shape channel
7 models, the performance of temperature uniformity can be potentially further improved.

8

5. Conclusions

This study proposed a novel approach introducing streamline concept to multi mini channel cooling plate to improve the overall cooling performance for Lithium-ion battery thermal management. The numerical simulation model has been studied and compared the results between the conventional straight channel plates and streamline channel cooling plates. The pressure difference, temperature difference, j/f factor and uniformity factor U_t of the multi mini channel cooling plates have been investigated. Main conclusions drawn from the study can be summarised as follows:

1. The flow can be effectively adjusted to smooth by adopting streamline shape channel models, which means the vortex and impacting flow could be avoided. Moreover, the entire flow resistance can be reduced by using the streamline shape channel plate.
2. The j/f factor representing the comprehensive performance of heat exchanger with streamline shape channels are significantly higher than that of typical straight channel models. Results indicated by using streamline mini channel models the j/f factor can be improved by 10.08% to 44.52%.
3. For the typical straight channel models, the flow resistance in the plates of even number channels is always higher than that of plates with odd number of channels. When the mass flow rate is 0.005 kg/s, the pressure drop can be as high as 6581 Pa and 6043 Pa with four and six typical straight channel number. When the streamline shape channels are used, the maximum pressure drop is only 3877 Pa. The streamline

1 shape channels can effectively reduce the pressure drop and avoid the direct flow
2 impaction, especially in the cooling plates with even number channels.

- 3 4. The temperature difference of streamline shape channel models with different
4 numbers of the channel is quite similar to that of typical straight 5 channel model,
5 which means the streamline channel models can keep the cooling ability at the same
6 level as the typical straight channel model. The effects of different numbers on the
7 cooling ability can be controlled by introducing a streamline shape concept to mini
8 channel cooling plate.

9 *Acknowledgement*

10 The authors would like to thank the supports from NSFC 91741203 to conduct the research
11 project. The financial support from Cao Guang Biao High Tech Talent Fund from Zhejiang
12 University is greatly acknowledged. The authors also would like to thank the support from
13 NSFC-RS Joint Project under the grant number no. 5151101443 and IE/151256.

14 *References*

- 15 [1] J. Du, D. Ouyang, Progress of Chinese electric vehicles industrialization in 2015: A review, *Applied Energy*,
16 188 (2017) 529-546.
17 [2] L. Rubino, C. Capasso, O. Veneri, Review on plug-in electric vehicle charging architectures integrated with
18 distributed energy sources for sustainable mobility, *Applied Energy*, 207 (2017) 438-464.
19 [3] S. Panchal, R. Khasow, I. Dincer, M. Agelin-Chaab, R. Fraser, M. Fowler, Thermal design and simulation of
20 mini-channel cold plate for water cooled large sized prismatic lithium-ion battery, *Applied Thermal Engineering*,
21 122 (2017) 80-90.
22 [4] H. Liu, Z. Wei, W. He, J. Zhao, Thermal issues about Li-ion batteries and recent progress in battery thermal
23 management systems: A review, *Energy Conversion and Management*, 150 (2017) 304-330.
24 [5] Q. Wang, B. Jiang, B. Li, Y.Y. Yan, A critical review of thermal management models and solutions of
25 lithium-ion batteries for the development of pure electric vehicles, *Renewable & Sustainable Energy Reviews*,
26 64 (2016) 106-128.
27 [6] A. Ritchie, W. Howard, Recent developments and likely advances in lithium-ion batteries, *Journal of Power*
28 *Sources*, 162 (2006) 809-812.

- 1 [7] Y.H. Ye, L.H. Saw, Y.X. Shi, A.A.O. Tay, Numerical analyses on optimizing a heat pipe thermal management
2 system for lithium-ion batteries during fast charging, *Applied Thermal Engineering*, 86 (2015) 281-291.
- 3 [8] J.Z. Xun, R. Liu, K. Jiao, Numerical and analytical modeling of lithium ion battery thermal behaviors with
4 different cooling designs, *Journal of Power Sources*, 233 (2013) 47-61.
- 5 [9] U.S. Kim, J. Yi, C.B. Shin, T. Han, S. Park, Modelling the thermal behaviour of a lithium-ion battery during
6 charge, *Journal of Power Sources*, 196 (2011) 5115-5121.
- 7 [10] B. Ravdel, K.M. Abraham, R. Gitzendanner, J. DiCarlo, B. Lucht, C. Campion, Thermal stability of lithium-ion
8 battery electrolytes, *Journal of Power Sources*, 119 (2003) 805-810.
- 9 [11] Y.H. Ye, Y.X. Shi, A.A.O. Tay, Electro-thermal cycle life model for lithium iron phosphate battery, *Journal of*
10 *Power Sources*, 217 (2012) 509-518.
- 11 [12] J. Jagemont, L. Boulon, Y. Dubé, A comprehensive review of lithium-ion batteries used in hybrid and
12 electric vehicles at cold temperatures, *Applied Energy*, 164 (2016) 99-114.
- 13 [13] Z.H. Rao, S.F. Wang, Y.L. Zhang, Simulation of heat dissipation with phase change material for cylindrical
14 power battery, *Journal of the Energy Institute*, 85 (2012) 38-43.
- 15 [14] Z.H. Rao, S.F. Wang, M.C. Wu, Z.R. Lin, F.H. Li, Experimental investigation on thermal management of
16 electric vehicle battery with heat pipe, *Energy Conversion and Management*, 65 (2013) 92-97.
- 17 [15] A.A. Pesaran, Battery thermal models for hybrid vehicle simulations, *Journal of Power Sources*, 110 (2002)
18 377-382.
- 19 [16] L.H. Saw, Y.H. Ye, A.A.O. Tay, W.T. Chong, S.H. Kuan, M.C. Yew, Computational fluid dynamic and thermal
20 analysis of Lithium-ion battery pack with air cooling, *Applied Energy*, 177 (2016) 783-792.
- 21 [17] R. Mahamud, C. Park, Reciprocating air flow for Li-ion battery thermal management to improve
22 temperature uniformity, *Journal of Power Sources*, 196 (2011) 5685-5696.
- 23 [18] S. Park, D.H. Jung, Battery cell arrangement and heat transfer fluid effects on the parasitic power
24 consumption and the cell temperature distribution in a hybrid electric vehicle, *Journal of Power Sources*, 227
25 (2013) 191-198.
- 26 [19] Y.L. Yang, X.S. Hu, D.T. Qing, F.Y. Chen, Arrhenius Equation-Based Cell-Health Assessment: Application to
27 Thermal Energy Management Design of a HEV NiMH Battery Pack, *Energies*, 6 (2013) 2709-2725.
- 28 [20] A. Jarrett, I.Y. Kim, Influence of operating conditions on the optimum design of electric vehicle battery
29 cooling plates, *Journal of Power Sources*, 245 (2014) 644-655.
- 30 [21] A. Jarrett, I.Y. Kim, Design optimization of electric vehicle battery cooling plates for thermal performance,
31 *Journal of Power Sources*, 196 (2011) 10359-10368.
- 32 [22] Z.Y. Ling, F.X. Wang, X.M. Fang, X.N. Gao, Z.G. Zhang, A hybrid thermal management system for lithium ion
33 batteries combining phase change materials with forced-air cooling, *Applied Energy*, 148 (2015) 403-409.
- 34 [23] Z.Y. Ling, J.J. Chen, X.M. Fang, Z.G. Zhang, T. Xu, X.N. Gao, S.F. Wang, Experimental and numerical
35 investigation of the application of phase change materials in a simulative power batteries thermal management
36 system, *Applied Energy*, 121 (2014) 104-113.
- 37 [24] K. Somasundaram, E. Birgersson, A.S. Mujumdar, Thermal-electrochemical model for passive thermal
38 management of a spiral-wound lithium-ion battery, *Journal of Power Sources*, 203 (2012) 84-96.
- 39 [25] Z.H. Rao, S.F. Wang, A review of power battery thermal energy management, *Renewable & Sustainable*
40 *Energy Reviews*, 15 (2011) 4554-4571.
- 41 [26] M.S. Wu, K.H. Liu, Y.Y. Wang, C.C. Wan, Heat dissipation design for lithium-ion batteries, *Journal of Power*
42 *Sources*, 109 (2002) 160-166.
- 43 [27] E.W. Lemmon, R.T. Jacobsen, Viscosity and thermal conductivity equations for nitrogen, oxygen, argon, and
44 air, *International Journal of Thermophysics*, 25 (2004) 21-69.

- 1 [28] T. Dixit, I. Ghosh, Review of micro- and mini-channel heat sinks and heat exchangers for single phase fluids,
2 Renewable & Sustainable Energy Reviews, 41 (2015) 1298-1311.
- 3 [29] B.H. Salman, H.A. Mohammed, K.M. Munisamy, A.S. Kherbeet, Characteristics of heat transfer and fluid
4 flow in microtube and microchannel using conventional fluids and nanofluids: A review, Renewable &
5 Sustainable Energy Reviews, 28 (2013) 848-880.
- 6 [30] P. Rosa, T.G. Karayiannis, M.W. Collins, Single-phase heat transfer in microchannels: The importance of
7 scaling effects, Applied Thermal Engineering, 29 (2009) 3447-3468.
- 8 [31] R. Mastrullo, A.W. Mauro, L. Viscito, Experimental CHF for low-GWP fluids and R134a. Effect of the L-h/D
9 ratio at low and high mass velocities, International Journal of Heat and Mass Transfer, 109 (2017) 1200-1216.
- 10 [32] Z.G. Qu, W.Q. Li, W.Q. Tao, Numerical model of the passive thermal management system for high-power
11 lithium ion battery by using porous metal foam saturated with phase change material, International Journal of
12 Hydrogen Energy, 39 (2014) 3904-3913.
- 13 [33] Z.H. Rao, S.F. Wang, G.Q. Zhang, Simulation and experiment of thermal energy management with phase
14 change material for ageing LiFePO₄ power battery, Energy Conversion and Management, 52 (2011) 3408-3414.
- 15 [34] J.T. Zhao, Z.H. Rao, Y.M. Li, Thermal performance of mini-channel liquid cooled cylinder based battery
16 thermal management for cylindrical lithium-ion power battery, Energy Conversion and Management, 103 (2015)
17 157-165.
- 18 [35] Y. Huo, Z. Rao, X. Liu, J. Zhao, Investigation of power battery thermal management by using mini-channel
19 cold plate, Energy Conversion and Management, 89 (2015) 387-395.
- 20 [36] Z. Qian, Y. Li, Z. Rao, Thermal performance of lithium-ion battery thermal management system by using
21 mini-channel cooling, Energy Conversion and Management, 126 (2016) 622-631.
- 22 [37] E. Tian, Y.L. He, W.Q. Tao, Numerical Simulation of Finned Tube Bank Across a Staggered
23 Circular-Pin-Finned Tube Bundle, Numerical Heat Transfer Part a-Applications, 68 (2015) 737-760.
- 24 [38] L.T. Tian, B. Liu, C.H. Min, J. Wang, Y.L. He, Study on the effect of punched holes on flow structure and heat
25 transfer of the plain fin with multi-row delta winglets, Heat and Mass Transfer, 51 (2015) 1523-1536.
- 26 [39] F.C. Chen, Z. Gao, R.O. Loutfy, M. Hecht, Analysis of Optimal Heat Transfer in a PEM Fuel Cell Cooling Plate,
27 Fuel Cells, 3 (2004) 181-188.
- 28 [40] S.M. Baek, S.H. Yu, J.H. Nam, C.J. Kim, A numerical study on uniform cooling of large-scale PEMFCs with
29 different coolant flow field designs, Applied Thermal Engineering, 31 (2011) 1427-1434.